Effective Passivation of Black Silicon Surfaces by Atomic Layer Deposition

Päivikki Repo, Antti Haarahiltunen, Lauri Sainiemi, Marko Yli-Koski, Heli Talvitie, Martin C. Schubert, and Hele Savin

***Abstract*—The poor charge-carrier transport properties attributed to nanostructured surfaces have been so far more detrimental for final device operation than the gain obtained from the reduced reflectance. Here, we demonstrate results that simultaneously show a huge improvement in the light absorption and in the surface passivation by applying atomic layer coating on highly absorbing silicon nanostructures. The results advance the development of photovoltaic applications, including high-efficiency solar cells or any devices, that require high-sensitivity light response.**

***Index Terms*—Aluminum oxide, atomic layer deposition (ALD), black silicon (b-Si), nanostructures.**

I. Introduction

BLACK silicon (b-Si) has been a subject of great interest in various fields, including photovoltaics [1]–[7], for its ability to reduce the surface reflectance even below 1%. However, many b-Si applications—especially solar cells—suffer from increased surface recombination, resulting in poor spectral response, especially at short wavelengths. This effect is often more detrimental for the final device operation than the gain from the reduced reflectance. Therefore, the key issue is clearly the surface passivation, which has been previously addressed by thermal oxidation. Thermal oxidation combined with b-Si and random pyramid texturing has resulted in 17.1% [6] solar cell efficiency, which could be improved by more effective surface passivation. More effective surface passivation methods are obviously needed to make black silicon a viable material for commercial applications including high-efficiency solar cells. In this paper, we present a method that provides extremely good surface passivation and simultaneously reduces the reflectance further at all wavelengths.

We solve the surface passivation problem with a conformal aluminum oxide (Al_2O_3) coating by atomic layer deposition (ALD). More than 3-ms lifetime values are measured in b-Si wafers by the quasi-steady-state photoconductance (QSSPC) and microwave photoconductance decay (μ-PCD) methods. Reflectance values of approximately 1% and below are reached in Al_2O_3 coated b-Si samples, indicating that besides reducing the surface recombination, the coating further suppresses the reflectance as well. Low reflectance values and effective passivation are also demonstrated in multicrystalline silicon wafers. All these results are very promising considering the use of b-Si surfaces, e.g., on solar cells to increase the efficiency to completely new levels.

Black silicon fabrication with reactive ion etching (RIE) was originally used for process optimization and black silicon as the outcome of the etching process was considered undesirable [8]. Today, numerous applications for b-Si besides photovoltaics have been suggested including microelectromechanical systems [9], ion mobility spectrometers [10], terahertz emitters [11], drug analysis [12], and photodetectors [13]. Black silicon surfaces can also be made superhydrophobic, which makes them self-cleaning [14]. Etching b-Si with RIE has certain advantages: It is fast and inexpensive and nanostructures can be made without mask layers [2]. Additionally, unlike wet etching approaches, in RIE, the etch rate is independent of crystalline planes. It should be emphasized although that the effective passivation method presented here is not most likely limited to the RIE-etched b-Si but could be applicable to other b-Si surfaces made by different technologies, as well, such as laser texturing [15] or metal-catalyzed wet chemical etching [16].

In recent years, Al_2O_3 has been widely studied as a surface passivation material for silicon-based photovoltaic applications [17]–[19]. The passivation ability of Al_2O_3 is related to the combination of low density of interface states and the fixed negative charge present in the material, which makes it especially promising for passivation of p-type emitters in n-type solar cells [20], [21]. ALD Al_2O_3 provides the lowest surface recombination velocities compared with Al_2O_3 deposited by other methods such as plasma-enhanced chemical vapor deposition or sputtering [22]. Because of the conformality and pinhole free nature [23], ALD is a natural choice for the coating of nanostructured b-Si surfaces.

II. Experimental Details

A. Sample Details and Black Silicon Etching

The first experiments were made on p-type magnetic (100) CZ-Si with resistivity of 2.7–3 Ω·cm, oxygen level 7–9 ppma, and 400-μm thickness. Four types of samples were prepared:

Manuscript received May 11, 2012; revised July 11, 2012; accepted July 16, 2012. Date of publication August 9, 2012; date of current version December 19, 2012. The work of P. Repo was supported by the Graduate School of the Faculty of Electronics, Communications and Automation. The work of L. Sainiemi was supported by the Academy of Finland under Grant 138674.

P. Repo, A. Haarahiltunen, M. Yli-Koski, H. Talvitie, and H. Savin are with the School of Electrical Engineering, Aalto University, FI-00076 Aalto, Finland (e-mail: paivikki.repo@aalto.fi; antti.haarahiltunen@aalto.fi; marko.yli-koski@aalto.fi; heli.talvitie@aalto.fi; hele.savin@aalto.fi).

L. Sainiemi was with the Division of Pharmaceutical Chemistry, University of Helsinki, 00014 Helsinki, Finland. He is now with Microsoft, 02150 Espoo, Finland (e-mail: lauri.sainiemi@live.fi).

M. C. Schubert is with the Fraunhofer Institute for Solar Energy Systems, 79110 Freiburg, Germany (e-mail: martin.schubert@ise.fraunhofer.de).

Color versions of one or more of the figures in this paper are available online at http://ieeexplore.ieee.org.

Digital Object Identifier 10.1109/JPHOTOV.2012.2210031

1) b-Si surface with Al_2O_3; 2) b-Si surface with thermal silicon dioxide (SiO_2); 3) flat (polished) surface with Al_2O_3; and 4) flat (polished) surface with thermal SiO_2. An identical set of samples was prepared on p-type (100) CZ-Si with resistivity of 17–24 Ω·cm, oxygen level 11–13 ppma, and 525-μm thickness. In addition, Al_2O_3 deposition was carried out on multicrystalline Si samples ($\sim$1 Ω·cm, thickness 200 μm), both with and without b-Si.

All black silicon surfaces were fabricated single-sidedly using a maskless cryogenic deep RIE process (Plasmalab System 100, Oxford Instruments, Abingdon, U.K.). The pieces of mc-Si wafers were glued on an Al_2O_3 coated silicon dummy wafer using photoresist prior to the etching. CZ-Si wafers were etched as such. The samples were cooled down to -120 °C and etched in SF_6/O_2 plasma for 7 min. The SF_6 and O_2 flow rates were set to 40 and 18 sccm, respectively, whereas the powers of inductively and capacitively coupled power sources were 1000 and 2 W, respectively. The process pressure was 10 mTorr. The mc-Si samples were detached from the dummy wafer in acetone after the etching process.

After b-Si etching, the wafers went through standard SC1 and SC2 cleaning and an HF-dip (HF: DIW 1:50) for 30 s. Wafers were dried in a rinse dryer in N_2 flow. Thermal oxidation was done at an oxidation furnace (Thermco 4104 TMX-9001) at 900 °C for 40 min followed by an anneal for 20 min, also at 900 °C. The resulting thermal oxide thickness measured with ellipsometry (Plasmos SD 2300) from a polished reference wafer was $\sim$15 nm.

B. Atomic Layer Deposited Al_2O_3

In this study, trimethylaluminum (TMA, $Al_2(CH_3)_6$) is chosen as the aluminum source and ozone (O_3) as the oxidant. This reactant combination is not as extensively studied as TMA+H_2O or plasma ALD if Al_2O_3 is deposited for surface passivation purposes [24], [25]. Although smaller growth per cycle (GPC) is achieved when O_3 is used, the larger reactivity of O_3 leads to a better film quality [26], which could also result in enhanced surface passivation properties.

Al_2O_3 was deposited on both sides of the wafers on a batch reactor with thermal ALD (Beneq TFS-500) at 200 °C. Reference samples with Al_2O_3 and SiO_2 but without b-Si were also processed alongside with the b-Si wafers. The resulting Al_2O_3 thickness of $\sim$23 nm was measured from these polished reference samples with ellipsometry. Postdeposition anneal (PEO-601/ATV) at 430 °C for 30 min in N_2 atmosphere was done for the Al_2O_3 samples to activate passivation.

III. Results and Discussion

A. Black Silicon Structure With Scanning Electron Microscopy

A scanning electron microscopy (SEM, Zeiss Supra 40) image of the Al_2O_3 coated b-Si sample is shown in Fig. 1(a) to give an idea of the surface structure and the dimensions on the surface. There is a slight variation in the dimensions of the b-Si pillars, the typical height being around 1 μm and diameter around 200 nm. The conformality of ALD on b-Si surfaces is shown in [27], where a thicker Al_2O_3 layer was deposited. In Fig. 1(a), the Al_2O_3 layer can be distinguished from the cross section as a lighter, narrow layer on top of the pillars. Fig. 1(b) shows a broader image of the mc-Si surface after b-Si etching, revealing a multiscale texture that originates from the initial surface roughness of mc-Si.

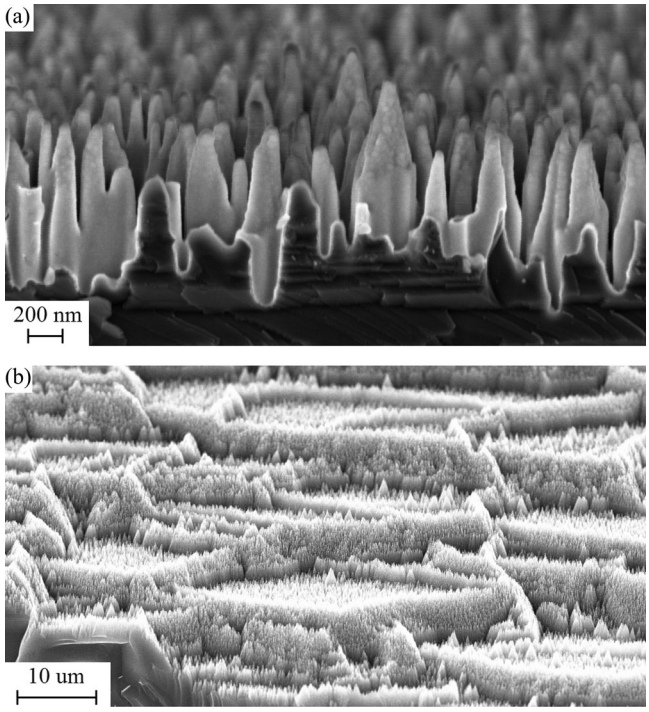

Fig. 1. SEM image of (a) the Al_2O_3 coated CZ Si surface with b-Si, where a thin Al_2O_3 layer can be seen on top of the nanostructure. (b) Noncoated mc-Si surface with b-Si.

B. Reflectance

The total reflectance of light on nanostructured low-resistivity CZ and mc-Si samples [see Fig. 2(a) and (b)] at the wavelength range of 250–1200 nm was measured using an Ulbricht sphere (Cary 500 Varian). The incident direction was close to the surface normal. As seen from the figure, reflectivity values are extremely low over a wide spectral range. This is typical behavior for b-Si due to the gradually varying refractive index from air to the substrate [28]. Moreover, the Al_2O_3 and SiO_2 coatings reduce the reflectance both in the CZ and mc samples, Al_2O_3 resulting in the lowest reflectance value. This is in agreement with the recent results by Otto *et al*. who showed that b-Si reflectance is reduced when the surface is coated with ALD aluminum-doped zinc oxide (ZnO:Al) [29]. The small difference in reflectance between the SiO_2 and Al_2O_3 coated samples can be attributed partly to the changes in the nanostructures caused by the thermal oxidation, whereas the thin and conformal ALD layer maintains the antireflection properties of the nanostructures. The differences in the refractive indices of SiO_2 and Al_2O_3 have also some effect. The lowest reflectance value of all samples, which is less than 0.85% in the whole wavelength range, is measured from the b-Si etched mc-Si sample coated

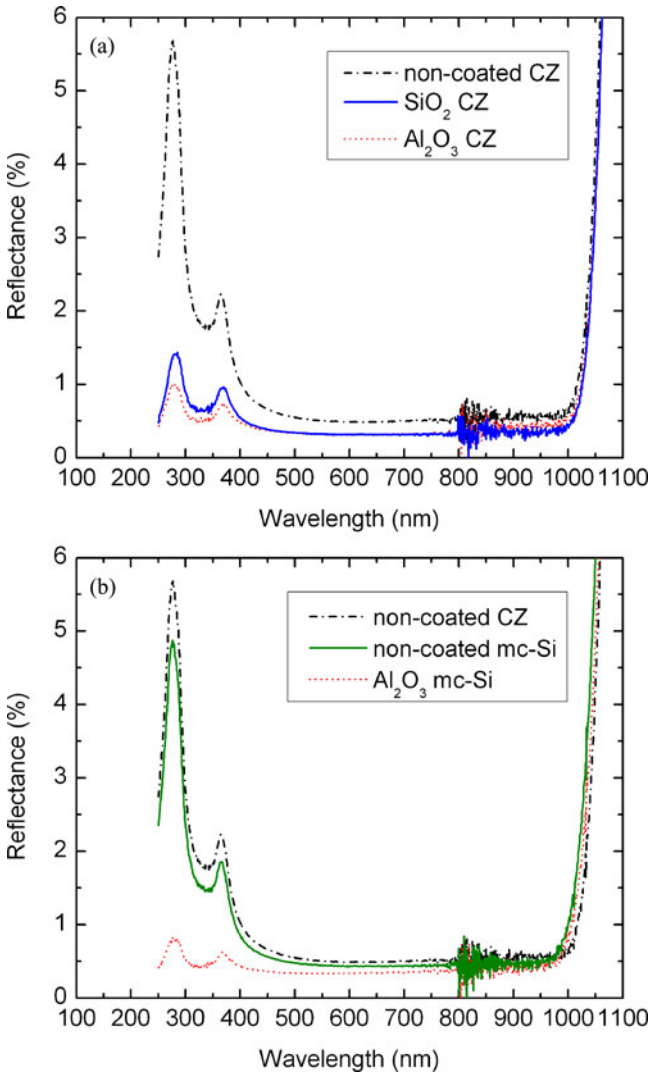

Fig. 2. Reflectance data of (a) low-resistivity CZ samples with noncoated, SiO_2 coated, and Al_2O_3 coated b-Si surfaces and (b) mc-Si samples with either noncoated or Al_2O_3 coated b-Si surfaces. In addition, the reflectance of the noncoated low-resistivity CZ sample is included in (b) for comparison.

with Al_2O_3 [see Fig. 2(b)]. This can be explained by the multiscale texture caused by the combination of the initial surface roughness of mc-Si and the b-Si etching [see Fig. 1(b)] [6]. The gained reflectance values are significantly better than the values obtained in commercial silicon nitride (SiN_x)-coated acid-textured mc-Si wafers or even the inverted pyramids used in high-efficiency silicon solar cells [30]. In addition, compared with the reflectance values of double-layer antireflection coatings, the reflectance of Al_2O_3 coated b-Si is smaller [31].

C. Minority Carrier Lifetimes

Fig. 3(a) and (b) shows the measured effective minority carrier lifetimes as a function of injection level in the low-resistivity and high-resistivity CZ samples, respectively. QSSPC measurements were done with Sinton Lifetime Tester (WCT-120) to determine the effective carrier lifetimes as a function of injection level. The optical constant that is needed as an input in the

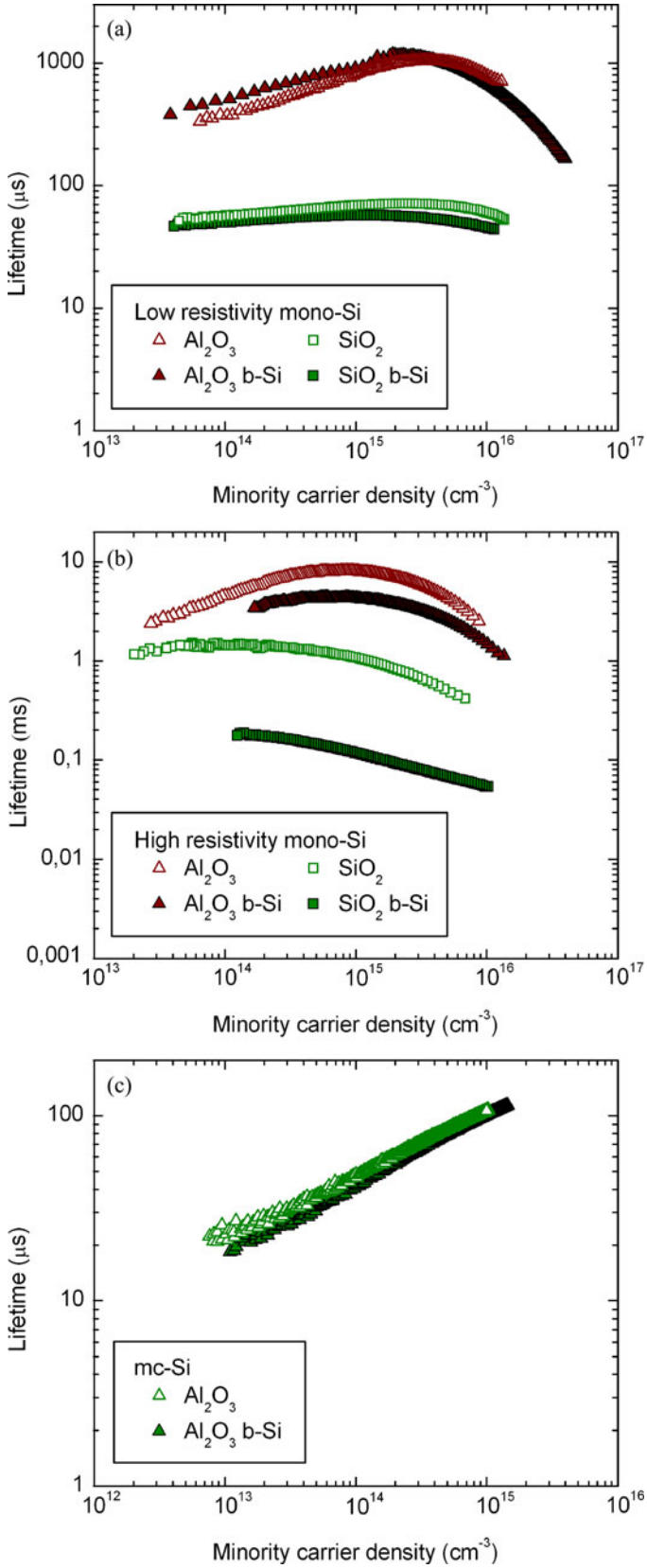

Fig. 3. Minority carrier lifetimes as a function of injection level of (a) the low-resistivity CZ samples, (b) high-resistivity CZ samples, and (c) mc-Si samples. CZ samples were measured with QSSPC and mc-Si with QSSPL. For CZ, four types of samples were processed: b-Si surfaces with Al_2O_3 and SiO_2 and, as a reference, similar samples but with polished surfaces. For mc-Si, two types of samples were prepared: Al_2O_3 coated mc-Si wafers with and without b-Si.

Sinton measurement was given the same value for both polished and b-Si etched samples. Depending on the film and its thickness, and the thickness of the wafer optical constant was given the value between 0.7–0.78. Corona charge was added on the thermally oxidized wafers before measurements.

Surprisingly, the passivation quality of Al_2O_3 on the b-Si surface is comparable with its passivation quality on the polished surface, and the measured lifetimes are in the millisecond range in all Al_2O_3 coated CZ samples. In the case of flat surface, the maximum surface recombination velocity can be calculated rather easily from the effective lifetime values by assuming an infinite carrier bulk lifetime [32]. With this assumption, the maximum surface recombination velocity S_{eff} for the reference samples can be calculated with the following equation:

$$S_{\text{eff}} = \frac{d}{2\tau_{\text{eff}}} \tag{1}$$

where d is the wafer thickness, and τ_{eff} is the measured effective lifetime at a certain injection level. Here, the injection level of 10^{15} cm^{-3} was chosen. The corresponding surface recombination velocities for polished samples are $S_{\max} = 25\,\text{cms}^{-1}$ in low-resistivity CZ and $S_{\max} = 3.3\,\text{cms}^{-1}$ in high-resistivity CZ. Surface recombination values in thermally oxidized samples are in all cases much higher.

With nanostructured surfaces, the maximum surface recombination velocity is an effective value. This means that the total recombination caused by the complicated nanostructure can be reduced to a flat plane just below the nanostructure using an effective surface recombination velocity [33]. In our case, only one surface was treated as a nanostructured surface and the other as a flat reference. Equation (1) is still valid for low-resistivity CZ as the lifetime of the Al_2O_3 coated b-Si wafers is as high or even higher than the lifetime of the polished reference wafers. Thus, from (1), the maximum surface recombination velocity for b-Si surface is $S_{\max} = 22\,\text{cms}^{-1}$. When assuming a zero surface recombination velocity on a flat surface [32], the correction for (1) is a factor of two in the case of Al_2O_3 coated low-resistivity CZ b-Si. This gives $S_{\max} = 13\,\text{cms}^{-1}$ for the corresponding high-resistivity CZ samples. Using surface recombination velocity $3.3\,\text{cms}^{-1}$ for a polished surface and diffusion constant 25 cm^{2}s^{-1} to solve numerically the equations given in [32], we get slightly smaller $S_{\max} = 9\,\text{cms}^{-1}$ for the Al_2O_3 coated high-resistivity CZ b-Si.

After verifying that the b-Si etching and the surface passivation with Al_2O_3 can be applied on p-type CZ material, the process was applied on p-type mc-Si wafers. Fig. 3(c) shows the minority carrier lifetimes as a function of injection level in two sister mc-Si wafers coated with Al_2O_3, both with and without the b-Si surface. There is no significant difference between the samples in lifetime, which indicates that Al_2O_3 can also passivate multicrystalline b-Si surfaces. The results were verified by μ-PCD (Semilab WT85XL-400). In addition, calibrated photoluminescence (PL) lifetime mapping and quasi-steady-state photoluminescence (QSSPL) [34] measurements were done for the mc-Si samples to omit the trapping effect and the uncertainty of the optical constant in QSSPC. Both methods lead to similar lifetimes for mc-Si with and without b-Si. Lifetimes of nearly 200 μs were reached in both cases when measured from corresponding good quality grains.

The reason why b-Si surfaces have been considered difficult to passivate is mainly related to the larger surface area attributed to the nanostructure. Xiong *et al*. have shown that the effective surface recombination velocity is directly proportional to the total surface area when the excess carrier distribution is uniform in the nanostructures [33]. The negative fixed charge related to Al_2O_3 decreases the excess carrier density in the nanostructures, which is probably the main reason for good passivation observed in the experiments. The same field-effect passivation is important in the case of flat surfaces but might be even more critical here as the charge prevents the electrons (minority carriers in p-Si) from reaching not only the surface but the entire nanostructure. The doping concentration, the formed space charge region, and the dimensions of the nanostructures also have an impact on this.

D. Discussion

p-type CZ and mc-Si wafers were used in the experiments reported here, but further studies are required to see if the method is also applicable on n-type and p+ with b-Si surfaces. Good Al_2O_3 passivation has been demonstrated on lowly doped n-type silicon where the passivation capability is partly due to the high negative charge, leading to an inversion layer [17], [18]. This relaxes the requirements on extremely low density of interface states [35]. The maximum surface recombination velocity occurs when surface charge causes a depletion of majority charge carriers (having attractive electric field for minority charge carriers) and when there is still relatively high majority charge-carrier concentration at the surface. Obviously, this can occur in n-type silicon with critical amount of fixed negative charge on the surface. If the surface charge density is well below this critical charge density, the surface recombination velocity is set by the density of interface states (or chemical passivation) [35]. However, if the surface charge density is well above the critical charge density, the surface recombination velocity is lowered due to the field effect [35]. Recently, this behavior was demonstrated for a phosphorus-doped emitter as implied open-circuit voltage went through the minimum when sheet resistance increased indicating rather good chemical passivation at higher doping levels and field effect at lower doping levels [36]. If n-type doping is so high that the field effect cannot be realized with Al_2O_3, the goal is to minimize the charge (or avoid maximum surface recombination) and maximize the chemical passivation. Unlike thermal oxidation, ALD is well known to have a good step coverage within small dimensions, which makes it a good candidate for b-Si passivation when only chemical passivation is considered.

IV. Conclusion

In summary, it has been demonstrated that ALD Al_2O_3 has the potential to be a material that effectively lowers the reflectivity and passivates black silicon surfaces, i.e., nanostructures that have less than 1% reflectance. Good surface passivation is crucial especially in photonic applications such as solar cells and photodetectors. Although ALD has been thought as a slow process, i.e., having a small GPC, large areas or multiple wafers can be coated at once, making ALD also feasible on an industrial

scale. The b-Si etching process used here is one possibility for low-cost, high-throughput fabrication because masking is not needed, and it is also suitable for multicrystalline samples. However, it can be assumed that the passivation method presented here is independent of the b-Si fabrication method.

ACKNOWLEDGMENT

The authors would like to thank E. Schäffer, J. Giesecke, L. Mundt, and M. Bühler from the Fraunhofer Institute for Solar Energy Systems for the PL, QSSPL, and reflectance measurements. P. Repo would like to thank S. Li and A. Perros for advice with ALD.

REFERENCES

[1] J. Li, H. Y. Yu, and Y. Li, "Aligned Si nanowire-based solar cells," *Nanoscale*, vol. 3, no. 12, pp. 4888–4900, Sep. 2011.

[2] L. Sainiemi, V. Jokinen, A. Shah, M. Shpak, S. Aura, P. Suvanto, and S. Franssila, "Non-reflecting silicon and polymer surfaces by plasma etching and replication," *Adv. Mater.*, vol. 23, no. 1, pp. 122–126, Oct. 2011.

[3] H.-C. Yuan, V. E. Yost, M. R. Page, P. Stradins, D. L. Meier, and H. M. Branz, "Efficient black silicon solar cell with a density-graded nanoporous surface: Optical properties, performance limitations, and design rules," *Appl. Phys. Lett.*, vol. 95, no. 12, pp. 123501-1–123501-3, Sep. 2009.

[4] S. Koynov, M. S. Brandt, and M. Stutzmann, "Black multi-crystalline silicon solar cells," *Phys. Status Solidi: Rapid Res. Lett.*, vol. 1, no. 2, pp. R53–R55, Oct. 2007.

[5] Y. Yan, H.-C. Yuan, V. E. Yost, K. Jones, M. Al-Jassim, and H. M. Branz, "Microstructure and surface chemistry of nanoporous "black silicon" for photovoltaics," in *Proc. 35th IEEE Photovoltaic Spec. Conf. Rec.*, Jun. 2010, pp. 2255–2257.

[6] F. Toor, H. M. Branz, M. R. Page, K. M. Jones, and H.-C. Yuan, "Multi-scale surface texture to improve blue response of nanoporous black silicon solar cells," *Appl. Phys. Lett.*, vol. 99, no. 10, pp. 103501-1–103501-3, Sep. 2011.

[7] C.-H. Lin, D. Z. Dimitrov, C.-H. Du, and C.-W. Lan, "Influence of surface structure on the performance of black-silicon solar cell," *Phys. Status Solidi*, vol. 7, no. 11–12, pp. 2778–2784, Sep. 2010.

[8] H. Jansen, M. de Boer, R. Legtenberg, and M. Elwenspoek, "The black silicon method: A universal method for determining the parameter setting of a fluorine-based reactive ion etcher in deep silicon trench etching with profile control," *J. Micromech. Microeng.*, vol. 5, no. 2, pp. 115–120, Jan. 1995.

[9] M. J. de Boer, J. G. E. (H.) Gardeniers, H. V. Jansen, E. Smulders, M.-J. Gilde, G. Roelofs, J. N. Sasserath, and M. Elwenspoek, "Guidelines for etching silicon MEMS structures using fluorine high-density plasmas at cryogenic temperatures," *J. Micromech. Microeng.*, vol. 11, no. 4, pp. 385–401, Aug. 2002.

[10] B. Gesemann, R. Wehrspohn, A. Hackner, and G. Müller, "Large-scale fabrication of ordered silicon nanotip arrays used for gas ionization in ion mobility spectrometers," *IEEE Trans. Nanotechnol.*, vol. 10, no. 1, pp. 50–52, Jan. 2011.

[11] P. Hoyer, M. Theuer, R. Beigang, and E.-B. Kley, "Terahertz emission from black silicon," *Appl. Phys. Lett.*, vol. 93, no. 9, pp. 091106-1–091106-3, Sep. 2008.

[12] L. Sainiemi, H. Keskinen, M. Aromaa, L. Luosujärvi, K. Grigoras, T. Kotiaho, J. M. Mäkelä, and S. Franssila, "Rapid fabrication of high aspect ratio silicon nanopillars for chemical analysis," *Nanotechnol.*, vol. 18, no. 50, pp. 505303-1–505303-7, Nov. 2007.

[13] Z. Huang, J. E. Carey, M. Liu, X. Guo, E. Mazur, and J. C. Campbell, "Microstructured silicon photodetector," *Appl. Phys. Lett.*, vol. 89, no. 3, pp. 033506-1–033506-3, Jul. 2006.

[14] J. Zhu, C.-M. Hsu, Z. Yu, S. Fan, and Y. Cui, "Nanodome solar cells with efficient light management and self-cleaning," *Nanolett.*, vol. 10, no. 6, pp. 1979–1984, Nov. 2010.

[15] M. Halbwax, T. Sarnet, Ph. Delaporte, M. Sentis, H. Etienne, F. Torregrosa, V. Vervisch, I. Perichaud, and S. Martinuzzi, "Micro and nano-structuration of silicon by femtosecond laser: Application to silicon photovoltaic cells fabrication," *Thin Solid Films*, vol. 516, no. 20, pp. 6791–6795, Dec. 2008.

[16] S. Koynov, M. S. Brandt, and M. Stutzmann, "Black nonreflecting silicon surfaces for solar cells," *Appl. Phys. Lett.*, vol. 88, no. 20, pp. 203107-1–203107-3, May 2006.

[17] B. Hoex, J. Schmidt, P. Pohl, M. C. M. van de Sanden, and W. M. M. Kessels, "Silicon surface passivation by atomic layer deposited Al_2O_3," *J. Appl. Phys.*, vol. 104, no. 4, pp. 044903-1–044903-12, Aug. 2008.

[18] G. Dingemans, R. Seguin, P. Engelhart, M. C. M. van de Sanden, and W. M. M. Kessels, "Silicon surface passivation by ultrathin Al_2O_3 films synthesized by thermal and plasma atomic layer deposition," *Phys. Status Solidi: Rapid Res. Lett.*, vol. 4, no. 1–2, pp. 10–12, Nov. 2010.

[19] J. Schmidt, B. Veith, and R. Brendel, "Effective surface passivation of crystalline silicon using ultrathin Al_2O_3 films and Al_2O_3/SiN_x stacks," *Phys. Status Solidi: Rapid Res. Lett.*, vol. 3, no. 9, pp. 287–289, Nov. 2009.

[20] J. Benick, B. Hoex, M. C. M. van de Sanden, W. M. M. Kessels, O. Schultz, and S. W. Glunz, "High efficiency n-type Si solar cells on Al_2O_3-passivated boron emitters," *Appl. Phys. Lett.*, vol. 92, no. 25, pp. 253504-1–253504-3, Jun. 2008.

[21] M. A. Green, K. Emery, Y. Hishikawa, and W. Warta, "Solar cell efficiency tables (version 35)," *Prog. Photovoltaics: Res. Appl.*, vol. 18, no. 2, pp. 144–150, Feb. 2010.

[22] J. Schmidt, F. Werner, B. Veith, D. Zielke, R. Bock, R. Brendel, V. Tiba, P. Poodt, F. Roozeboom, A. Li, and A. Cuevas, "Surface passivation of silicon solar cells using industrially relevant Al_2O_3 deposition techniques," *Photovoltaics Int.*, vol. 10, pp. 52–57, 2010.

[23] J. L. van Hemmen, S. B. S. Heil, J. H. Klootwijk, F. Roozeboom, C. J. Hodson, M. C. M. van de Sanden, and W. M. M. Kessels, "Plasma and thermal ALD of Al_2O_3 in a commercial 200 mm ALD reactor," *J. Electrochem. Soc.*, vol. 154, no. 7, pp. G165–G169, May 2007.

[24] P. Repo, H. Talvitie, S. Li, J. Skarp, and H. Savin, "Silicon Surface Passivation by Al_2O_3: Effect of ALD reactants," *Energy Procedia*, vol. 8, pp. 681–687, Apr. 2011.

[25] G. Dingemans, N. M. Terlinden, D. Pierreux, H. B. Profijt, M. C. M. van de Sanden, and W. M. M. Kessels, "Influence of the oxidant on the chemical and field-effect passivation of Si by ALD Al_2O_3," *Electrochem. Solid-State. Lett.*, vol. 14, no. 1, pp. H1–H4, Oct. 2011.

[26] S.-C. Ha, E. Choi, S.-H. Kim, and J. S. Roh, "Influence of oxidant source on the property of atomic layer deposited Al_2O_3 on hydrogen-terminated Si substrate," *Thin Solid Films*, vol. 476, no. 2, pp. 252–257, Oct. 2005.

[27] L. Sainiemi, K. Grigoras, and S. Franssila, "Suspended nanostructured alumina membranes," *Nanotechnol.*, vol. 20, no. 7, pp. 075306-1–075306-6, Jan. 2009.

[28] P. B. Clapham and M. C. Hutley, "Reduction of lens reflexion by the "moth-eye" principle," *Nature*, vol. 244, no. 5414, pp. 281–282, Aug. 1973.

[29] M. Otto, M. Kroll, T. Käsebier, S.-M. Lee, M. Putkonen, R. Salzer, P. T. Miclea, and R. B. Wehrspohn, "Conformal transparent conducting oxides on black silicon," *Adv. Mater.*, vol. 22, no. 44, pp. 5035–5038, Sep. 2010.

[30] D. H. Macdonald, A. Cuevas, M. Kerr, C. Samundsett, D. Ruby, S. Winderbaum, and A. Leo, "Texturing industrial multicrystalline silicon solar cells," *Solar Energy*, vol. 76, no. 1–3, pp. 277–283, Aug. 2004.

[31] J. Zhao, A. Wang, P. P. Altermatt, S. R. Wenham, and M. A. Green, "24% efficient Perl solar cell: Recent improvements in high efficiency silicon cell research," *Solar Energy Mater. Solar Cells*, vol. 41, pp. 87–99, Jun. 1999.

[32] A. B. Sproul, "Dimensionless solution of the equation describing the effect of surface recombination on carrier decay in semiconductors," *J. Appl. Phys.*, vol. 76, no. 5, pp. 2851–2854, Sep. 1994.

[33] K. Xiong, S. Lu, D. Jiang, J. Dong, and H. Yang, "Effective recombination velocity of textured surfaces," *Appl. Phys. Lett.*, vol. 96, no. 19, pp. 193107-1–193107-3, May 2010.

[34] J. A. Giesecke, M. C. Schubert, D. Walter, and W. Warta, "Minority carrier lifetime in silicon wafers from quasi-steady-state photoluminescence," *Appl. Phys. Lett.*, vol. 97, no. 9, pp. 092109-1–092109-3, Sep. 2010.

[35] B. Hoex, J. J. H. Gielis, M. C. M. van de Sanden, and W. M. M. Kessels, "On the c-Si surface passivation mechanism by the negative-charge-dielectric Al_2O_3," *J. Appl. Phys.*, vol. 104, pp. 113703-1–113703-7, Dec. 2008.

[36] B. Hoex, M. C. M. van de Sanden, J. Schmidt, R. Brendel, and W. M. M. Kessels, "Surface passivation of phosphorus-diffused n^+-type emitters by plasma-assisted atomic-layer deposited Al_2O_3," *Phys. Status Solidi: Rapid Res. Lett.*, vol. 6, no. 1, pp. 4–6, Oct. 2011.

Authors' photographs and biographies not available at the time of publication.